Spectroscopic Characteristics of Indium Nitride Nanoparticles Prepared by Pulsed Laser Ablation

Saad A. Lafi

Department of Physics, College of Science, University of Misan, Amara, IRAQ

Abstract
In this work, pulsed laser ablation was used to prepare indium nitride nanoparticles and their spectroscopic characteristics were determined and analyzed. An Nd:YAG laser was used to irradiate an indium target immersed in ammonium hydroxide solution using different laser energies (40, 60, 80, and 100mJ) at different ablation times (5, 10 and 15 min). The transmittance of the prepared nanoparticles was studied as a function of both laser energy used for irradiation and ablation time.

Keywords: Indium nitride; Nanoparticles; Laser ablation; Spectroscopic characteristics
Received: 15 April 2024; **Revised:** 10 May 2024r; **Accepted:** 17 May 2024; **Published:** 1 July 2024

1. Introduction

During the last few years the interest in the indium nitride (InN) semiconductor has been notice. Indium nitride is an important III-nitride semiconductor with many potential applications [1,2]. The main problems in creating InN are low dissociation temperature of InN [3,4], relatively low melting point of indium metal [5,6], the mismatched with the substrate, and the difficulty in achieving good material quality [7]. In spite of all these problems, InN has taken a lot of attention as a potential material for manufacturing high speed optoelectronic devices [8,9]. It owns good electron transport properties, low effective electron mass and comprises a surface electron accumulation layer, which make it a suitable material for the fabrication of high frequency devices [10-12]. Low effective mass for electrons which leads to high mobility and high saturation velocity [13]. It was found that InN offers high peak drift velocity at room temperature [14]. The direct and narrow-band gap [15], high thermal conductivity, excellent mechanical properties, high electrical resistance, and its piezoelectric constants are relatively large make indium nitride taking special interesting [16,17].

The quality and performance of the InN based device structures are dependent on the crystal structure. InN crystallize in the following categorize: wurtzite (hexagonal), zincblende (cubic) [18]. InN crystallizes in the hexagonal wurtzite lattice that consists of two hexagonal close packed (HCP) sub-lattices of In and N atoms in C^4_{6V} symmetry. Juza and Hahn first reported the crystalline structure of InN to be wurtzite. The WZ structure is usually represented by two lattice parameters *a* and *c*. The basic lattice constants are a = 3.5365 Å and c = 5.70399 Å [19]. In this structure each atom is four-fold coordinated. The strong uniaxial nature in combination with the partially ionic bonding leads to a strong piezoelectric polarization along the c-axis [20].

In this work, pulsed laser ablation was used to prepare indium nitride nanoparticles and their spectroscopic characteristics were determined and analyzed.

2. Experimental Part

Figure (1) shows the experimental setup for laser ablation of indium target immersed in ammonium hydroxide (NH_4OH) (24.5%) solution, which includes laser source: HUAFEI Nd:YAG laser system (λ=1064nm) with maximum energy per pulse of 1000 mJ, pulse width of 10 ns, repetition rate of 1 Hz. The laser is applied with a lens of 120 mm focal length to increase the laser fluence.

A pure indium target (HIMEDIA, 99.99%), with dimensions of 5x10x1mm^3

was used in this work as a target material for the preparation of indium nitride nanoparticles. The ablation process was typically done for ablation times of 5, 10 and 15 min at room temperature with different energies (40, 60, 80 and 100mJ). The target placed in a sealed stainless steel container.

The sealed stainless steel cell was made up of three sections strongly bolted together. A glass window was placed on the top of the cell to prevent splashing of the liquid phase and hence loss of ablated materials. The experiments ablation of the indium target in ammonium hydroxide in this work was carried out in the sealed cell.

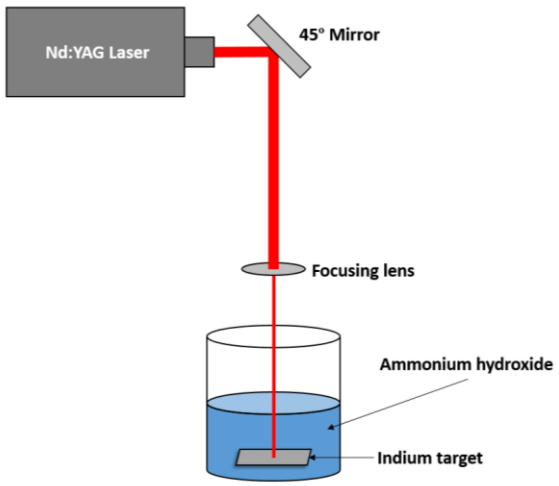

Fig. (1) The experimental setup for the preparation of indium nitride nanoparticles

3. Results and Discussion

Figure (2) demonstrates the influence of varying the laser energy and ablation time on nanoparticle concentration generated by laser ablation of indium target at different conditions. The laser energy at range from 40 to 100 mJ and varying laser ablation time (5 to 15min) illustrated in this figure. Figure (2a) demonstrates the influence of the ablation time of laser ablation of indium target (5, 10 and 15 min) at 80 mJ; the nanoparticles concentration increased almost linearly with laser ablation time. It was clearly observed that the increase laser ablation time between 10 and 15 min allows higher particle concentration production. Increase the concentration of the indium nitride nanoparticles in the case of laser ablation in liquid is related to increased radiation absorbed by the material due to increased beam absorption. As expected, the material removal rate, strongly depends on of laser ablation time. When increasing the laser ablation time, this will lead to increase the overlapping pulses.

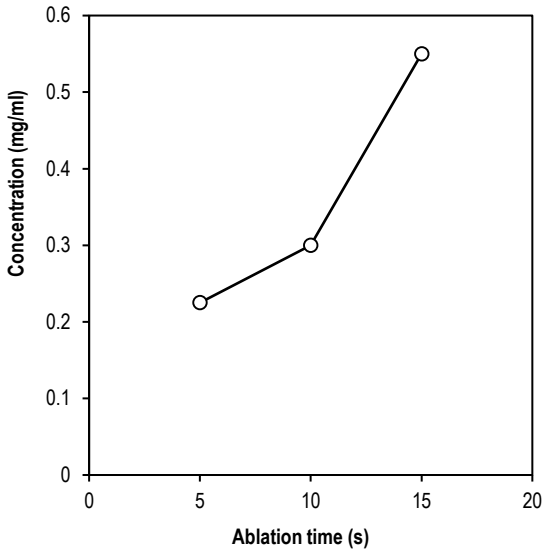

(a)

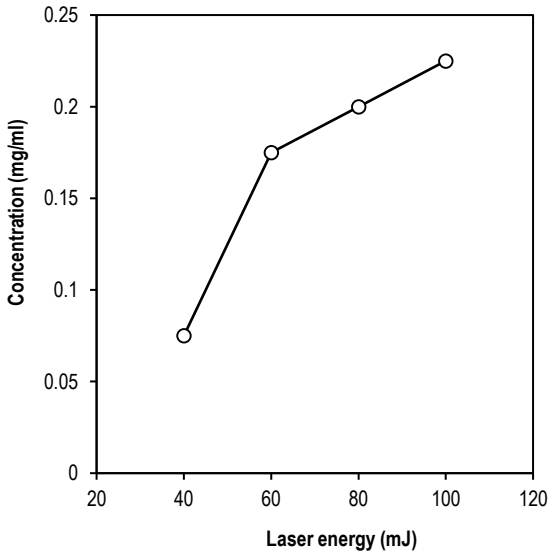

(b)

Fig. (2) Variation of InN nanoparticles concentration as a function of (a) ablation time, and (b) laser energy

Figure (2b) introduce the effect of changing laser energy on the concentration of the particle. As observed, the laser energy increased from 40 mJ to higher value, the ablation efficiency enhanced. Delivering more energy that implies ablating larger amount of material because of the plasma

plume becomes more intense and the nanoparticles cloud becomes denser.

Production of InN can be confirmed most easily by UV-Vis-NIR spectroscopy through the assignment of the characteristic transmission peaks which reflect the lengths of InN. The effect of the laser energy on the formation of InN nanoparticles is very important. Figure (3) shows UV-visible-IR transmission spectra of suspensions of InN nanoparticles prepared by laser ablation of an indium target in ammonium hydroxide at different laser energies (40, 60, 80, and 100 mJ) at a constant laser ablation time (5 min). The height and width of the transmission spectra were found to be dependent upon the laser energy. It can be clearly seen that the transmission peak intensity decrease with the laser energy increased due to increase of the InN concentration. The maximum optical transmission edge at 1378 nm, the all sample spectra show the similar peaks, but each line has different absorbance value in each point of the wavelength. This indicates that the InN nanoparticles produced have different size of distribution.

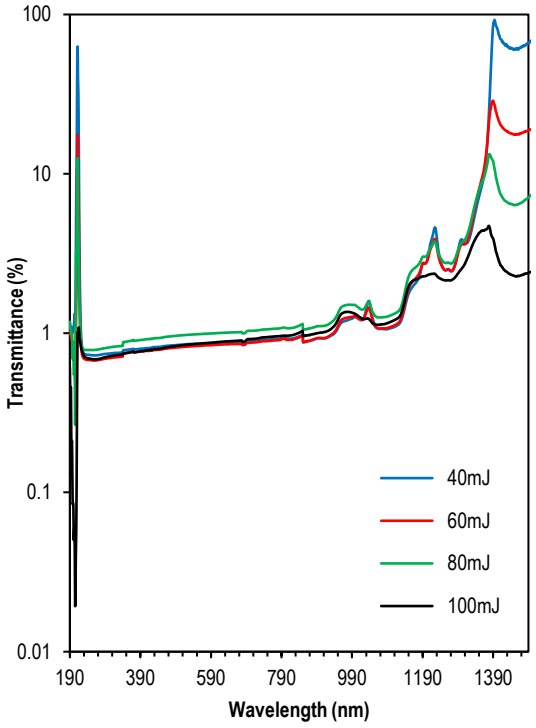

Fig. (3) UV-visible-IR transmission spectra of the samples prepared using different laser energies at constant ablation time (5 min)

The narrower peak on the spectrum indicates the more homogenous size distribution. The height of the peak is calculated from the based line of spectrum, spectrum 80mj and 100mj and shows lowest transmittance that indicates the highest number of InN NPs in solution. Spectra of 40 and 60 mJ show higher transmittance most probably that is because the spectrum has more number of big particles in the solution that reflect much more light than the spectra of 80 and 100mJ. Also the intensity of InN produced change with laser energy; figure (3) explain these effects are due to the change of nanoparticles concentration with laser energy.

4. Conclusions

In this work, pulsed laser ablation was used to prepare indium nitride nanoparticles and their spectroscopic characteristics were determined and analyzed. The transmittance of the prepared nanoparticles was studied as a function of both laser energy used for irradiation and ablation time. It can be concluded that using higher laser energy lead to decrease the transmittance of the prepared nanoparticles as the concentration of these nanoparticles is consequently increased.

References

[1] W.F. Lim, Z. Hassan and H.J. Quah, "Structural, morphological, optical, and gas sensing characteristics of ultraviolet-assisted photoelectrochemical etching derived AlInGaN nano-spikes", J. Mater. Res. Technol., 8(3) (2019) 2767-2776.

[2] W. Nabgan et al., "A bibliometric examination and state-of-the-art overview of hydrogen generation from photoelectrochemical water splitting", Int. J. Hydro. Ener., 52(A) (2024) 358-380.

[3] J. Zhang et al., "Tandem internal electric fields in intralayer/interlayer carbon nitride homojunction with a directed flow of photo-excited electrons for photocatalysis", Appl. Catal. B: Enviro. Ener., 333 (2023) 122781.

[4] X. Li et al., "Boosting photocatalytic degradation of RhB via interfacial electronic effects between Fe-based ionic liquid and g-C_3N_4", Green Ener. Enviro., 4(2) (2019) 198-206.

[5] M. Krekorian et al., "Characterization of Intrinsically Radiolabeled Poly(lactic-co-

glycolic acid) Nanoparticles for ex Vivo Autologous Cell Labeling and in Vivo Tracking", Bioconj. Chem., 32(8) (2021) 1802-1811.

W. Nabgan et al., "A review on the design of nanostructure-based materials for photoelectrochemical hydrogen generation from wastewater: Bibliometric analysis, mechanisms, prospective, and challenges", Int. J. Hydro. Ener., 52(C) (2024) 622-663.

[6] S. Yuan et al., "Two-dimensional layered materials for modifying solid-state electrolytes in lithium batteries via interface engineering", Mater. Design, 235 (2023) 112425.

[7] M. Liu et al., "Tuning the core-shell ratio in nanostructured CuS@In2S3 photocatalyst for efficient dye degradation", Clean. Chem. Eng., 5 (2023) 100093.

[8] Y. Wang et al., "A Single-Junction Cathodic Approach for Stable Unassisted Solar Water Splitting", Joule, 3(10) (2019) 2444-2456.

[9] L. Abad-Gil and C.M.A. Brett, "Poly(methylene blue)-ternary deep eutectic solvent/Au nanoparticle modified electrodes as novel electrochemical sensors: Optimization, characterization and application", Electrochimica Acta, 434 (2022) 141295.

[10] J.-Y. Sui et al., "Design and research of the Janus metastructure", Resul. Phys., 61 (2024) 107795.

[11] O. Gohar et al., "Nanomaterials for advanced energy applications: Recent advancements and future trends", Mater. Design, 241 (2024) 112930.

[12] R. Kumar Mishra et al., "Nanomaterial integration in micro LED technology: Enhancing efficiency and applications", Next Nanotech., 5 (2024) 100056.

[13] C. Erkmen et al., "Layer-by-layer modification strategies for electrochemical detection of biomarkers", Biosens. Bioelectron. X, 12 (2022) 100270.

[14] F.-X. Xie et al., "Enhancement of visible light photocatalytic pharmaceutical degradation and hydrogen evolution of Bi_5O_7Br by in situ disorder engineering", Trans. Nonferr. Metals Soc. China, 33(6) (2023) 1862-1872.

[15] N. Mansor et al., "Graphitic Carbon Nitride as a Catalyst Support in Fuel Cells and Electrolyzers", Electrochimica Acta, 222 (2016) 44-57.

[16] A.G.-M. Ferrari et al., "Electroanalytical overview: The detection of chromium", Sens. Actuat. Rep., 4 (2022) 100116.

[17] L. Liu et al., "Ni and ZrO_2 promotion of In_2O_3 for CO_2 hydrogenation to methanol", Appl. Catal. B: Enviro. Ener., 356 (2024) 124210.

[18] K. Han et al., "Research on photoelectrochemical photodetectors based on bismuth 2d thin films", Opt. Mater., 148 (2024) 114971.

[19] H. Yang et al., "Carbon nitride of five-membered rings with low optical bandgap for photoelectrochemical biosensing", Chem, 7(10) (2021) 2708-2721.

[20] K.M. Cannon et al., "Working with lunar surface materials: Review and analysis of dust mitigation and regolith conveyance technologies", Acta Astronautica, 196 (2022) 259-274.

